

This article was downloaded by: [Renmin University of China]

On: 13 October 2013, At: 10:34

Publisher: Taylor & Francis

Informa Ltd Registered in England and Wales Registered Number: 1072954 Registered office: Mortimer House, 37-41 Mortimer Street, London W1T 3JH, UK



Journal of Coordination Chemistry

Publication details, including instructions for authors and subscription information:

<http://www.tandfonline.com/loi/gcoo20>

Synthesis, characterization, photocleavage, cytotoxicity in vitro, apoptosis, and cell cycle arrest of ruthenium(II) complexes

Qi-Feng Guo^a, Si-Hong Liu^a, Qing-Hua Liu^a, Hui-Hua Xu^a, Jian-Hua Zhao^a, Hai-Feng Wu^a, Xin-Yan Li^a & Jian-Wei Wang^a

^a Department of Orthopaedics, Guangzhou First Municipal People's Hospital Affiliated to Guangzhou Medical College, Guangzhou 510180, PR China

Published online: 03 May 2012.

To cite this article: Qi-Feng Guo, Si-Hong Liu, Qing-Hua Liu, Hui-Hua Xu, Jian-Hua Zhao, Hai-Feng Wu, Xin-Yan Li & Jian-Wei Wang (2012) Synthesis, characterization, photocleavage, cytotoxicity in vitro, apoptosis, and cell cycle arrest of ruthenium(II) complexes, Journal of Coordination Chemistry, 65:10, 1781-1791, DOI: [10.1080/00958972.2012.680592](https://doi.org/10.1080/00958972.2012.680592)

To link to this article: <http://dx.doi.org/10.1080/00958972.2012.680592>

PLEASE SCROLL DOWN FOR ARTICLE

Taylor & Francis makes every effort to ensure the accuracy of all the information (the "Content") contained in the publications on our platform. However, Taylor & Francis, our agents, and our licensors make no representations or warranties whatsoever as to the accuracy, completeness, or suitability for any purpose of the Content. Any opinions and views expressed in this publication are the opinions and views of the authors, and are not the views of or endorsed by Taylor & Francis. The accuracy of the Content should not be relied upon and should be independently verified with primary sources of information. Taylor and Francis shall not be liable for any losses, actions, claims, proceedings, demands, costs, expenses, damages, and other liabilities whatsoever or howsoever caused arising directly or indirectly in connection with, in relation to or arising out of the use of the Content.

This article may be used for research, teaching, and private study purposes. Any substantial or systematic reproduction, redistribution, reselling, loan, sub-licensing, systematic supply, or distribution in any form to anyone is expressly forbidden. Terms &

Conditions of access and use can be found at <http://www.tandfonline.com/page/terms-and-conditions>

Synthesis, characterization, photocleavage, cytotoxicity *in vitro*, apoptosis, and cell cycle arrest of ruthenium(II) complexes

QI-FENG GUO*, SI-HONG LIU, QING-HUA LIU, HUI-HUA XU,
JIAN-HUA ZHAO, HAI-FENG WU, XIN-YAN LI and JIAN-WEI WANG

Department of Orthopaedics, Guangzhou First Municipal People's Hospital Affiliated to
Guangzhou Medical College, Guangzhou 510180, PR China

(Received 8 December 2011; in final form 28 February 2012)

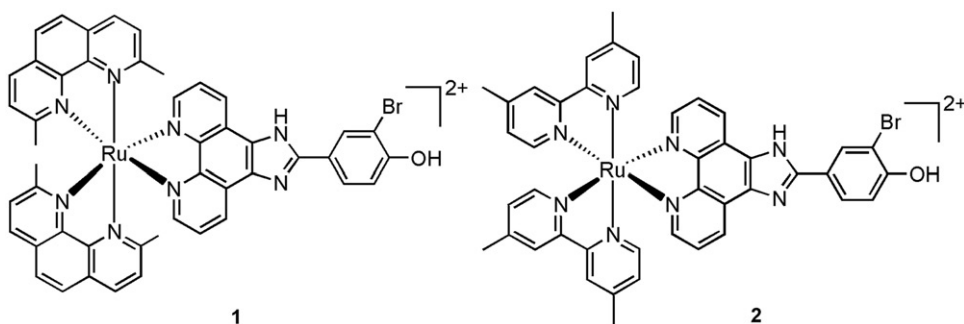
Two new ruthenium(II) complexes, $[\text{Ru}(\text{dmp})_2(\text{BHIP})]^{2+}$ (**1**) and $[\text{Ru}(\text{dmb})_2(\text{BHIP})]^{2+}$ (**2**), were synthesized and characterized by elemental analysis, ESI-MS, and ^1H NMR. DNA-binding constants of these complexes with calf-thymus DNA (*ct*-DNA) were determined to be $2.09 (\pm 0.18) \times 10^4 (\text{mol L}^{-1})^{-1}$ ($s = 2.58$) and $1.48 (\pm 0.17) \times 10^5 (\text{mol L}^{-1})^{-1}$ ($s = 1.57$), respectively. Viscosity measurements show that **1** and **2** interact with *ct*-DNA by intercalation. Upon irradiation at 365 nm, **1** and **2** induce cleavage of pBR322 DNA. The cytotoxicity of these complexes was evaluated by 3-(4,5-dimethylthiazol-2-yl)-2,5-diphenyltetrazolium bromide (MTT) assay. The apoptosis induced by the complexes was studied by flow cytometry. The results of the cell cycle arrest show that **2** can inhibit the proliferation of BEL-7402 cells in the G0/G1 phase.

Keywords: Ruthenium(II) complexes; Photocleavage; Cytotoxicity; Apoptosis; Cell cycle arrest

1. Introduction

Interaction of ruthenium(II) complex with DNA has been extensively studied [1–10]. In general, Ru(II) polypyridyl complexes bind DNA with non-covalent interactions such as electrostatic binding, groove binding, and intercalation. Many ruthenium(II) complexes show unique properties, $[\text{Ru}^{\text{II}}(\text{tpy})(\text{pic})(\text{H}_2\text{O})]^+$ can induce DNA cleavage in the presence of KHSO_5 [11], $[\text{Ru}(\text{Melm})(\text{iip})]^{2+}$ [12] can induce uncoiling of calf-thymus DNA (*ct*-DNA), $[\text{Ru}(\text{phen})_2(\text{APIP})]^{2+}$ [13], and $[\text{Ru}(\text{dmb})_2(\text{pdpt})]^{2+}$ [14] show high antioxidant activity against hydroxyl radical. Studies on bioactivity of ruthenium(II) complexes have also been examined [15]. $[(3\text{-Py})\text{Ru}(\text{phen})_2(\text{tmopp})]^+$ can effectively inhibit the proliferation of HepG-2 cells with a low IC_{50} value ($18.7 \pm 1.3 \mu\text{g mL}^{-1}$) [16], $[\eta^6\text{-C}_6\text{Me}_6\text{RuCl}(\text{dppz})](\text{CF}_3\text{SO}_3)$ shows high cytotoxicity to MCF-7 cells ($\text{IC}_{50} = 2.1 \pm 0.6 \mu\text{mol L}^{-1}$) [17], $[\text{Ru}(\text{dip})_2(\text{dcdppz})]^{2+}$ can induce the apoptosis of BEL-7402 cells [18], and $[\text{Ru}(\text{bpy})_2(\text{DNPIP})]^{2+}$ suggests the antiproliferative mechanism on HepG-2 was S-phase arrest [18]. In this article, a new ligand, BHIP, was synthesized. This ligand has one more bromide than HPIP [19]. To evaluate the

*Corresponding author. Email: qifengguoqf@126.com

Scheme 1. The structures of **1** and **2**.

effect of Br on bioactivity, two new ruthenium(II) polypyridyl complexes, $[\text{Ru}(\text{dmp})_2(\text{BHIP})]^{2+}$ (**1**) (dmp = 2,9-dimethyl-1,10-phenanthroline, BHIP = 2-(3-bromo-4-hydroxyphenyl)imidazo[4,5-f][1,10]phenanthroline) and $[\text{Ru}(\text{dmb})_2(\text{BHIP})]^{2+}$ (**2**) (dmb = 4,4'-dimethyl-2,2'-bipyridine, scheme 1), were synthesized and characterized by elemental analysis, electrospray ionization mass spectrometry (ESI-MS), and ^1H NMR. Their DNA-binding behaviors were investigated by electronic absorption titration, viscosity measurements, and photocleavage. The cytotoxicity of these complexes against BEL-7402, Hela, MCF-7, and MG-63 cells were evaluated by 3-(4,5-dimethylthiazol-2-yl)-2,5-diphenyltetrazolium bromide (MTT). The apoptosis of BEL-7402 cells induced by **1** and **2** was investigated by flow cytometry. The cell cycle arrest was also studied.

2. Materials and methods

2.1. Synthesis of ligand and complexes

2.1.1. Synthesis of BHIP. A mixture of 1,10-phenanthroline-5,6-dione (0.315 g, 1.5 mmol) [20], 3-bromo-4-hydroxyphenylaldehyde (0.302 g, 1.5 mmol), ammonium acetate (2.31 g, 30 mmol), and glacial acetic acid (30 mL) was refluxed with stirring for 2 h. The cooled solution was diluted with water and neutralized with concentrated aqueous ammonia. The precipitate was collected and purified by column chromatography on silica gel (60–100 mesh) with ethanol as eluent to give the compound as yellow powder. Yield: 80%. Anal. Calcd for $\text{C}_{19}\text{H}_{11}\text{N}_4\text{BrO}$: C, 58.33; H, 2.83; N, 14.32; Found (%): C, 58.18; H, 2.95; N, 14.47. FAB-MS: $m/z = 392.3$ $[\text{M} + 1]^+$. ^1H NMR (500 MHz, $\text{DMSO}-d_6$): 9.92 (d, 2H, $J = 6.0$ Hz), 8.89 (d, 2H, H_i , $J = 8.0$ Hz), 8.41 (d, 1H, $J = 2.5$ Hz), 7.22 (d, 1H, $J = 6.5$ Hz), 7.82 (dd, 2H, $J = 4.5$, $J = 4.5$ Hz), 7.15 (d, 1H, $J = 8.0$ Hz), 3.40 (s, 1H, $H_{\text{O-H}}$).

2.1.2. Synthesis of $[\text{Ru}(\text{dmp})_2(\text{BHIP})]^{2+}$ (1**).** A mixture of *cis*- $[\text{Ru}(\text{dmp})_2\text{Cl}_2] \cdot 2\text{H}_2\text{O}$ (0.260 g, 0.5 mmol) [21] and BHIP (0.196 g, 0.5 mmol) in ethanol (30 mL) was refluxed under argon for 8 h to give a clear red solution. Upon cooling, a red precipitate was

obtained by dropwise addition of saturated aqueous NaClO₄ solution. The crude product was purified by column chromatography on neutral alumina oxide with a mixture of CH₃CN–toluene (3:1, v/v) as eluent. The red band was collected. The solvent was removed under reduced pressure and a red powder was obtained. Yield: 71%. Anal. Calcd for C₄₇H₃₅BrCl₂N₈O₉Ru: C, 50.96; H, 3.18; N, 10.12. Found (%): C, 50.55; H, 2.94; N, 10.51. ESI-MS [CH₃CN, *m/z*]: 907.6 ([M–2ClO₄–H]⁺), 454.5 ([M–2ClO₄]²⁺). ¹H NMR (500 MHz, DMSO-*d*₆): δ 8.89 (d, 2H, *J* = 8.4 Hz), 8.82 (d, 2H, *J* = 8.3 Hz), 8.40 (t, 4H, *J* = 8.0 Hz), 8.36 (d, 1H, *J* = 2.1 Hz), 8.22 (d, 2H, *J* = 8.8 Hz), 8.08 (d, 1H, *J* = 2.1 Hz), 7.96 (d, 2H, *J* = 8.4 Hz), 7.43 (dd, 2H, *J* = 5.5, *J* = 5.5 Hz), 7.35 (d, 2H, *J* = 8.4 Hz), 7.26 (d, 2H, *J* = 5.1 Hz), 7.08 (d, 1H, *J* = 8.6 Hz), 3.35 (s, 1H, H_{O–H}), 2.06 (s, 6H), 1.93 (s, 6H).

2.1.3. Synthesis of [Ru(dmb)₂(BHIP)]²⁺ (2). This complex was synthesized in a manner identical to that described for **1**, with *cis*-[Ru(dmb)₂Cl₂]·2H₂O (0.280 g, 0.5 mmol) [22] in place of *cis*-[Ru(dmp)₂Cl₂]·2H₂O. Yield: 72%. Anal. Calcd for C₄₃H₃₅BrCl₂N₈O₉Ru: C, 48.74; H, 3.33; N, 10.57. Found (%): C, 48.55; H, 3.44; N, 10.72. ESI-MS [CH₃CN, *m/z*]: 859.3 ([M–2ClO₄–H]⁺), 430.5 ([M–2ClO₄]²⁺). ¹H NMR (500 MHz, DMSO-*d*₆): δ 9.03 (d, 2H, *J* = 7.6 Hz), 8.69 (d, 4H, *J* = 8.5 Hz), 8.45 (d, 1H, *J* = 2.0 Hz), 8.16 (d, 1H, *J* = 2.1 Hz), 8.01 (d, 2H, *J* = 5.5 Hz), 7.87 (dd, 2H, *J* = 5.3, *J* = 5.3 Hz), 7.38 (dd, 4H, *J* = 6.4, *J* = 5.9 Hz), 7.14 (d, 2H, *J* = 7.0 Hz), 6.99 (d, 1H, *J* = 8.6 Hz), 3.35 (s, 1H, H_{O–H}), 2.12 (s, 6H), 2.07 (s, 6H).

Caution: Perchlorate salts of metal compounds with organic ligands are potentially explosive, and only small amounts of the material should be prepared and handled with great care.

2.2. Physical measurements

ct-DNA was obtained from the Sino-American Biotechnology Company. pBR322 DNA was obtained from Shanghai Sangon Biological Engineering & Services Co., Ltd. Dimethyl sulfoxide (DMSO) and RPMI 1640 were purchased from Sigma. Cell lines of hepatocellular origin (BEL-7402), human epithelial carcinoma (Hela), breast cancer (MCF-7), and human osteosarcoma (MG-63) were purchased from American Type Culture Collection, agarose and ethidium bromide were obtained from Aldrich. RuCl₃·*x*H₂O was purchased from Kunming Institution of Precious Metals. 1,10-Phenanthroline was obtained from Guangzhou Chemical Reagent Factory. Doubly-distilled water was used to prepare buffers (5 mmol L^{–1}) tris(hydroxymethyl)aminomethane-HCl (Tris-HCl), 50 mmol L^{–1} NaCl, pH = 7.2). A solution of *ct*-DNA in the buffer gave a ratio of UV absorbance at 260 nm and 280 nm of *ca* 1.8–1.9:1, indicating that the DNA was sufficiently free of protein [23]. The DNA concentration per nucleotide was determined by absorption spectroscopy using the molar absorption coefficient (6600 (mol L^{–1})^{–1} cm^{–1}) at 260 nm [24].

Microanalysis (C, H, and N) was carried out with a Perkin-Elmer 240Q elemental analyzer. Fast atom bombardment (FAB) mass spectra were recorded on a VG ZAB-*HS* spectrometer in a 3-nitrobenzyl alcohol matrix. ESI-MS were recorded on a LCQ system (Finnigan MAT, USA) using methanol as mobile phase. The spray voltage, tube lens offset, capillary voltage, and capillary temperature were set at 4.50 kV, 30.00 V,

23.00 V, and 200°C, respectively, and the quoted m/z values are for the major peaks in the isotope distribution. ^1H NMR spectra were recorded on a Varian-500 spectrometer. All chemical shifts were given relative to tetramethylsilane. UV-Vis spectra were recorded on a Shimadzu UV-3101PC spectrophotometer at room temperature.

2.3. DNA-binding and photoactivated cleavage

The DNA-binding and photoactivated cleavage experiments were performed at room temperature. Buffer A (5 mmol L⁻¹ Tris hydrochloride, 50 mmol L⁻¹ NaCl, pH 7.0) was used for absorption titration, luminescence titration, and viscosity measurements. Buffer B (50 mmol L⁻¹ Tris-HCl, 18 mmol L⁻¹ NaCl, pH 7.2) was used for DNA photocleavage experiments.

The absorption titrations of the complex in buffer were performed using a fixed concentration (20 μmol L⁻¹) for complex to which increments of the DNA stock solution were added. Ru-DNA solutions were allowed to incubate for 5 min before absorption spectra were recorded. The intrinsic binding constants K , based on the absorption titration, were measured by monitoring changes in absorption at the metal-to-ligand charge transfer (MLCT) band with increasing concentration of DNA according to the literature [25].

Viscosity measurements were carried out using an Ubbelodhe viscometer maintained at 25.0 (±0.1)°C in a thermostatic bath. DNA samples approximately 200 base pairs in average length were prepared by sonication to minimize complexities arising from DNA flexibility [26]. The relative viscosities were measured [27, 28] and the data were treated with the same methods reported by Cohen [29].

For the gel electrophoresis experiment, supercoiled pBR322 DNA (0.1 μg) was treated with the Ru(II) complexes in buffer B, and the solution was then irradiated at room temperature with a UV lamp (365 nm, 10 W) for 45 min. The samples were analyzed by electrophoresis for 1.5 h at 80 V on a 0.8% agarose gel in TBE (89 mmol L⁻¹ Tris-borate acid, 2 mmol L⁻¹ EDTA, pH=8.3). The gel was stained with 1 μg mL⁻¹ ethidium bromide and photographed on an Alpha Innotech IS-5500 fluorescence chemiluminescence and visible imaging system.

2.4. Cytotoxicity assay

Standard MTT assay procedures were used [30]. Cells were placed in 96-well microassay culture plates (8 × 10³ cells per well) and grown overnight at 37°C in a 5% CO₂ incubator. The complexes tested were dissolved in DMSO and diluted with RPMI 1640 and then added to the wells to achieve final concentrations ranging from 10⁻⁶ to 10⁻⁴ mol L⁻¹. Control wells were prepared by addition of culture medium (100 μL). Wells containing culture medium without cells were used as blanks. The plates were incubated at 37°C in a 5% CO₂ incubator for 48 h. Upon completion of the incubation, stock MTT dye solution (20 μL, 5 mg mL⁻¹) was added to each well. After 4 h incubation, buffer (100 μL) containing DMF (50%) and sodium dodecyl sulfate (20%) was added to solubilize the MTT formazan. The optical density of each well was then measured on a microplate spectrophotometer at a wavelength of 490 nm. The IC₅₀ values were determined by plotting the percentage of viability *versus* concentration on a logarithmic graph and reading off the concentration at which 50% of the cells remain

viable relative to the control. Each experiment was repeated at least three times to get the mean values. Four different tumor cell lines were the subjects of this study: BEL-7402, Hela, MCF-7, and MG-63 (purchased from American Type Culture Collection).

2.5. Apoptotic assay by flow cytometry

After chemical treatment, 1×10^6 cells were harvested, washed with phosphate buffer saline (PBS), then fixed with 70% ethanol, and finally maintained at 4°C for at least 12 h. Then the pellets were stained with the fluorescent probe solution containing $50 \mu\text{g mL}^{-1}$ propidium iodide (PI) and 1 mg mL^{-1} annexin in PBS on ice in the dark for 15 min. Then the fluorescence emission was measured at 530 nm and 575 nm (or equivalent) using 488 nm excitation by a FACS Calibur flow cytometer (Beckman Dickinson & Co., Franklin Lakes, NJ). A minimum of 10,000 cells were analyzed per sample.

2.6. Cell cycle arrest

BEL-7402 cells were seeded into six-well plates (Costar, Corning Corp, New York) at a density of 2×10^5 cells per well and incubated for 24 h. The cells were cultured in RPMI 1640 supplemented with 10% of fetal bovine serum and incubated at 37°C and 5% CO₂. The medium was removed and replaced with medium (final DMSO concentration, 1% v/v) containing the complex ($25 \mu\text{mol L}^{-1}$). After incubation for 24 h, the cell layer was trypsinized and washed with cold PBS and fixed with 70% ethanol. Twenty mL of RNase (0.2 mg mL^{-1}) and 20 mL of PI (0.02 mg mL^{-1}) were added to the cell suspensions and incubated at 37°C for 30 min. Then the samples were analyzed by a FACS Calibur flow cytometer (Beckman Dickinson & Co., Franklin Lakes, NJ). The number of cells analyzed for each sample was more than 10^4 [31].

3. Results and discussion

3.1. Synthesis and characterization

BHIP was synthesized with a method similar to that described by Steck and Day [32]. Complexes **1** and **2** were prepared by refluxing BHIP with *cis*-[Ru(dmp)₂Cl₂]·2H₂O or *cis*-[Ru(dmb)₂Cl₂]·2H₂O in ethanol. The structures of the ligand and its complexes were confirmed by elemental analysis, FAB-MS, ES-MS, and ¹H NMR. The chemical shifts of protons on nitrogen of imidazole were not observed, probably because the protons are very active and easily exchanged between the two nitrogen atoms of imidazole in solution. In the ESI-MS spectra for **1** and **2**, as expected, intense signals for [M-2ClO₄-H]⁺ and [M-2ClO₄]²⁺ were observed; the obtained molecular weights were consistent with the expected values.

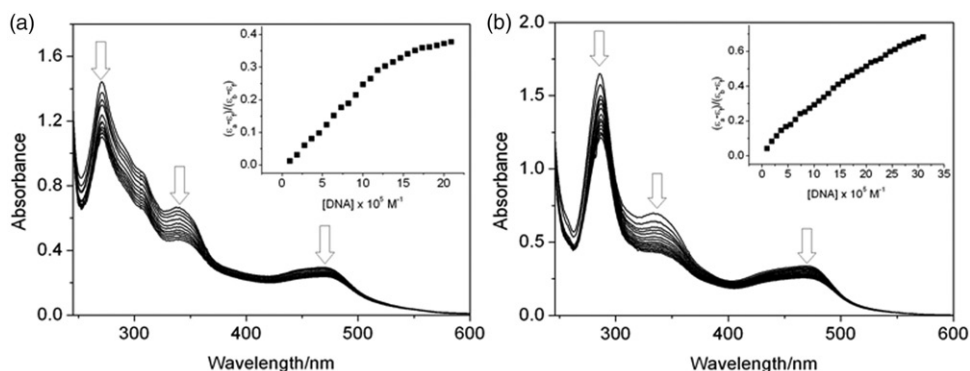


Figure 1. Absorption spectra of complexes in Tris-HCl buffer upon addition of *ct*-DNA in the presence of (a) **1** and (b) **2**. $[\text{Ru}] = 20 \mu\text{mol L}^{-1}$. Arrows show the absorbance change upon increase of DNA concentration. Plots of $(\epsilon_a - \epsilon_f)/(\epsilon_b - \epsilon_f)$ vs. $[\text{DNA}]$ for titration of DNA with Ru(II) complexes.

3.2. Electronic absorption titration

In the presence of increasing amounts of *ct*-DNA, absorption spectra of **1** and **2** are shown in figure 1. The hypochromism of the MLCT band of **1** at 468 nm and **2** at 467 nm upon binding to DNA are 26.78% and 28.19% with 2 and 3 nm red shifts, respectively. These spectral characteristics suggest that these complexes interact with DNA most likely through a mode that involves a stacking interaction between the aromatic chromophore and the base pairs of DNA. DNA-binding constants were obtained by monitoring the changes in absorbance at the MLCT band with increasing concentration of DNA. The intrinsic binding constants were determined to be $2.09 (\pm 0.18) \times 10^4 (\text{mol L}^{-1})^{-1}$ ($s = 2.58$) and $1.48 (\pm 0.17) \times 10^5 (\text{mol L}^{-1})^{-1}$ ($s = 1.57$), respectively. These values are smaller than those of $[\text{Ru}(\text{bpy})_2(\text{dppz})]^{2+}$ ($> 10^6 (\text{mol L}^{-1})^{-1}$) [33], but comparable to those of DNA intercalators $[\text{Ru}(\text{dmp})_2(\text{HAPIP})]^{2+}$ (HAPIP = 2-(2-hydroxyl-5-aminophenyl)imidazo[4,5-f][1,10]phenanthroline, $3.30 \times 10^4 (\text{mol L}^{-1})^{-1}$) [34], $[\text{Ru}(\text{dmb})_2(\text{BFIP})]^{2+}$ (BFIP = 2-benzo[b]furan-2-yl-1H-imidazo[4,5-f][1,10]phenanthroline, $3.20 \times 10^4 (\text{mol L}^{-1})^{-1}$) [35], and $[\text{Ru}(\text{dmb})_2(\text{ITAP})]^{2+}$ (ITAP = Isatino[1,2-b]-1,4,8,9-tetraazatriphenylene, $4.50 \times 10^4 (\text{mol L}^{-1})^{-1}$) [36]. The difference between the two intrinsic constants is caused by different ancillary ligands. Complex **1** shows less binding strength to *ct*-DNA. Substitution on 2- and 9-positions of the ancillary phen ligands must cause severe steric constraints near the core of Ru(II) when the complex intercalates into the DNA base pairs. The methyl groups may come into close proximity of base pairs at the intercalative site. These steric clashes prevent the complex from intercalating effectively, decreasing the intrinsic constant. Such steric interactions would not be present with substitution on the 4- and 4'-positions of ancillary bpy ligands [37].

3.3. Viscosity measurements

Changes in relative viscosity of DNA solutions have proven useful for assignment of mode of binding to DNA. The relative change in viscosity was measured using *ct*-DNA

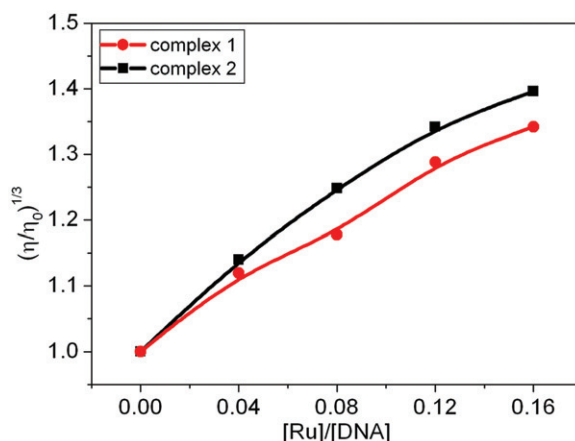


Figure 2. Effect of increasing amounts of **1** (●) and **2** (■) on the relative viscosity of *ct*-DNA at 25 (±0.1)°C. [DNA] = 0.25 mmol L⁻¹.

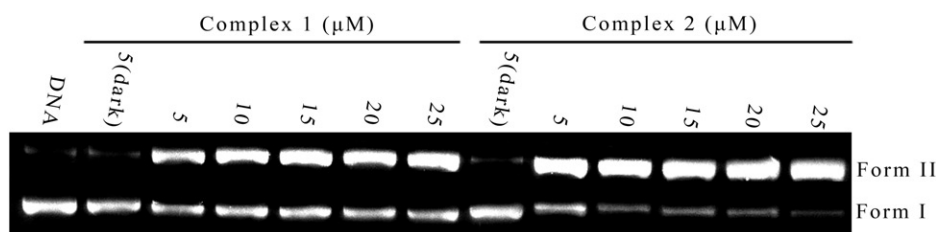


Figure 3. Photoactivated cleavage of pBR322 DNA in the presence of different complexes upon irradiation at 365 nm for 45 min.

with increasing concentrations of **1** and **2**. The effect of **1** and **2** on the relative viscosity of rod-like DNA are shown in figure 2. On increasing concentrations of **1** and **2**, the relative viscosity of DNA solution increased steadily. These results suggest that **1** and **2** intercalate between the base pairs of *ct*-DNA. Enhancements of the relative viscosity of DNA follow the order $2 > 1$, consistent with the DNA-binding affinities.

3.4. Photocleavage of pBR322 DNA

When circular plasmid DNA is subjected to electrophoresis, relatively fast migration will be observed for the intact supercoil form (Form I); if scission occurs on one strand (nicking), the supercoil will relax to generate a slower-moving open circular form (Form II) [38]. The gel electrophoresis separation of pBR322 DNA after incubation with the Ru(II) complexes and irradiation at 365 nm for 45 min is shown in figure 3. No obvious DNA cleavage was observed for controls in which complexes were absent or incubation of the plasmid with the Ru(II) complex in dark. Both complexes exhibited concentration-dependent, single-strand cleavage of supercoiled Form I to nicked Form II. At increasing concentration of the Ru(II) complexes, the amount of Form I of pBR322 DNA diminishes gradually, whereas that of Form II increases. Comparing the

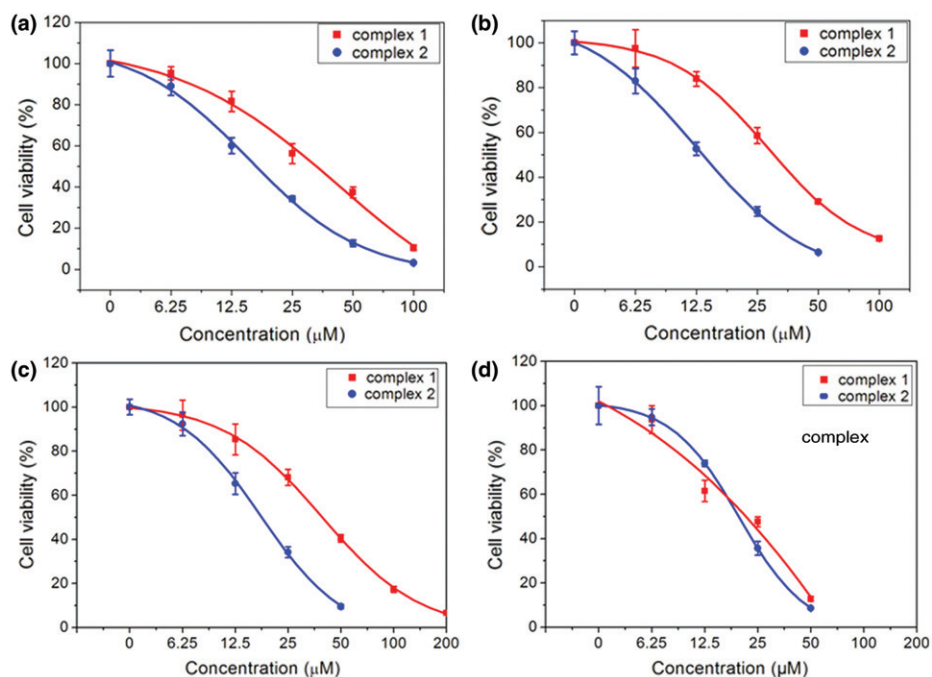


Figure 4. Cell viability of **1** and **2** on BEL-7402 (a), HeLa (b), MCF-7 (c), and MG-63 (d) cell proliferation *in vitro*. Each point is obtained from three independent experiments with the mean \pm standard error.

effect on cleavage of pBR322 DNA, **2** exhibits more effective DNA cleavage than **1**. This may be attributed to the different DNA-binding affinity of two Ru(II) complexes.

3.5. Cytotoxicity *in vitro*

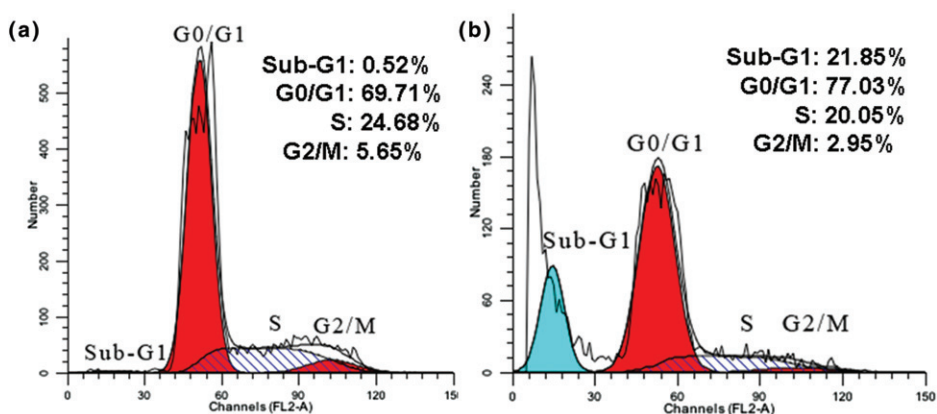
The cytotoxicity *in vitro* of Ru(II) complexes was determined against BEL-7402, HeLa, MCF-7, and MG-63 cell lines using the MTT assay. Due to low aqueous solubility, **1** and **2** were dissolved in DMSO and blank samples containing the same amount of DMSO were used as controls. The cell viability is depicted in figure 4. The cytotoxicity of complexes was concentration-dependent. The cell viability decreased with increasing concentrations of **1** and **2**. The IC_{50} values were calculated (table 1). Both complexes demonstrate high *in vitro* cytotoxicity against selected tumor cell lines. Comparing IC_{50} values of **1** and **2**, **2** appeared to be more active than **1** against all the cell lines, consistent with the DNA-binding affinities of **1** and **2**. Comparing the IC_{50} values of these complexes with that of $[Ru(phen)_2(HPIP)]^{2+}$ ($> 100 \mu mol L^{-1}$) on BEL-7402 cells [19], owing to the Br in HPIP, the cytotoxicities of **1** and **2** were largely enhanced.

3.6. Apoptosis assay by flow cytometer

In order to gain insight into the type of cell death induced by **1** and **2**, apoptotic assays on BEL-7402 cells were investigated by cell apoptosis analyses and the percentage of

Table 1. The IC₅₀ values of **1** and **2** against selected cell lines.

Complex	IC ₅₀ (μmol L ⁻¹)			
	BEL-7402	Hela	MCF-7	MG-63
1	25.5	27.8	39.4	19.4
2	16.9	13.2	16.5	17.1

Figure 5. Cell cycle distribution of BEL-7402 cells as analyzed by FACS caliber flow cytometry. Control (a), exposed to **2** (25 μmol L⁻¹, (b) for 24 h.

apoptotic and necrotic cells determined by flow cytometry. In the control (a), the percentage of apoptotic (A) and necrotic (N) cells were 0.20% and 0.09%, respectively. In the presence of **1** (b) and **2** (c) (Supplementary material), the percentage of apoptosis (A) and necrosis (N) of BEL-7402 cells was 37.64% and 7.33% for **1** and 16.52% and 0.46% for **2**. Cell apoptosis increased by 37.44% and 16.32% at 25 μmol L⁻¹. However, the ratios of apoptosis *versus* necrosis are 5.14 and 35.91 for **1** and **2**, respectively. Comparing the ratios under identical conditions, **2** shows higher apoptotic effect than **1**. These results are consistent with those obtained from the IC₅₀ values.

3.7. Cell cycle arrest

Studies on ruthenium complex-induced anti-proliferative action on cancer cells have attracted much attention [39–41]. Complex **2** was chosen for investigating cell cycle arrest as it showed higher cytotoxicity than **1** towards all cell lines. Induction of apoptosis of cells can inhibit cancer cell proliferation. After treatment of BEL-7402 cells with **2** for 24 h, the cell cycle of BEL-7402 cells was investigated by flow cytometry in PI-stained cell method. Figure 5 shows that treatment of BEL-7402 cells with **2** caused an increase at G₀/G₁ phase, accompanied by corresponding reduction in the percentage of cells in S phase. The percentage of enhancement in G₀/G₁ phase was 7.32%. In addition, the percentage of apoptosis (sub-G₁) also shows an enhancement of 21.33%.

These data suggest that the antiproliferative mechanism on BEL-7402 cells was a *G0/G1* phase arrest and apoptosis.

4. Conclusions

Two new ruthenium(II) complexes, $[\text{Ru}(\text{dmp})_2(\text{BHIP})]^{2+}$ (**1**) and $[\text{Ru}(\text{dmb})_2(\text{BHIP})]^{2+}$ (**2**), were synthesized and characterized. Viscosity measurements suggest that **1** and **2** interact with *ct*-DNA by intercalation. Under identical conditions, **2** showed more effective DNA cleavage than **1**. The results from cytotoxicity assay show that **2** exhibits higher cytotoxic activity than **1** against selected tumor cell lines. The apoptotic assay demonstrates that **2** showed more effective apoptosis of BEL-7402 cells than **1**. For **1** and **2**, bioactivities are consistent with the DNA-binding affinities. Additionally, **2** can inhibit the proliferation of BEL-7402 cells in the *G0/G1* phase.

Acknowledgments

This work was supported by the Science and Technology Foundation of Guangdong Province (No. 2010B31500005), Science and Technology Planning Project Pillar Program of Guangzhou Municipality (No. 2010J-E021-1), and Medical Scientific Research Foundation of Guangzhou Municipality (201102A212029) of China.

References

- [1] O. Novakova, J. Malina, T. Suchankova, J. Kasparikova, T. Bugarcic, P.J. Sadler, V. Brabec. *Chem. – Eur. J.*, **16**, 5744 (2010).
- [2] B. Sun, J.X. Guan, L. Xu, J.F. Kou, L. Wang, X.D. Ding, H. Chao, L.N. Ji. *Inorg. Chem.*, **48**, 4637 (2009).
- [3] Y.J. Liu, H. Chao, Y.X. Yuan, H.J. Yu, L.N. Ji. *Inorg. Chim. Acta*, **359**, 3807 (2006).
- [4] O. Novakova, H.M. Chen, O. Vrana, A. Rodger, P.J. Sadler, V. Brabec. *Biochemistry*, **42**, 11544 (2003).
- [5] S. Shi, X.T. Geng, J. Zhao, T.M. Yao, C.R. Wang, D.J. Yang, L.F. Zheng, L.N. Ji. *Biochimie*, **92**, 370 (2010).
- [6] Y.J. Liu, Y.Y. Wei, F.H. Wu, W.J. Mei, L.X. He. *Spectrochim Acta, Part A*, **70**, 171 (2008).
- [7] L.F. Tan, J.L. Shen, X.J. Chen, X.L. Liang. *DNA Cell Biol.*, **28**, 461 (2009).
- [8] A. Sigel, H. Sigel (Eds). In *Metal Ions in Biological Systems*, Vol. 33, Marcel Dekker, New York (1996).
- [9] K.E. Erkkila, D.T. Odom, J.K. Barton. *Chem. Rev.*, **99**, 2777 (1999).
- [10] L.N. Ji, X.H. Zou, J.G. Liu. *Coord. Chem. Rev.*, **216–217**, 513 (2001).
- [11] D. Chatterjee, A. Sengupta, R.V. Eldik. *J. Coord. Chem.*, **64**, 30 (2011).
- [12] X.C. Yang, Y.N. Liu, S.T. Yao, Y. Xia, Q. Li, W.J. Zhen, L.M. Chen, J. Liu. *J. Coord. Chem.*, **64**, 1491 (2011).
- [13] Y.J. Liu, Z.H. Liang, Z.Z. Li, J.H. Yao, H.L. Huang. *J. Organomet. Chem.*, **696**, 2729 (2011).
- [14] H.L. Hong, Z.H. Liang, M.H. Zeng. *J. Coord. Chem.*, **64**, 3792 (2011).
- [15] L. Salassa. *Eur. J. Inorg. Chem.*, 4931 (2001).
- [16] Y.N. Liu, X.N. Zhang, R. Zhang, T.F. Chen, Y.S. Wong, J. Liu, W.J. Zheng. *Eur. J. Inorg. Chem.*, 1974 (2011).
- [17] S. Schäfer, I. Ott, R. Gust, W.S. Sheldrick. *Eur. J. Inorg. Chem.*, 3034 (2007).
- [18] H.L. Huang, Z.Z. Li, Z.H. Liang, Y.J. Liu. *Eur. J. Med. Chem.*, **46**, 3282 (2011).
- [19] J. Liu, W.J. Zheng, S. Shi, C.P. Tan, J.C. Chen, K.C. Zheng, L.N. Ji. *J. Inorg. Biochem.*, **102**, 193 (2008).
- [20] M. Yamada, Y. Tanaka, Y. Yoshimoto, S. Kuroda, I. Shimao. *Bull. Chem. Soc. Jpn.*, **65**, 1006 (1992).

- [21] J.P. Collin, J.P. Sauvage. *Inorg. Chem.*, **25**, 135 (1986).
- [22] B.P. Sullivan, D.J. Salmon, T.J. Meyer. *Inorg. Chem.*, **17**, 3334 (1978).
- [23] J. Marmur. *J. Mol. Biol.*, **3**, 208 (1961).
- [24] M.E. Reichmann, S.A. Rice, C.A. Thomas, P. Doty. *J. Am. Chem. Soc.*, **76**, 3047 (1954).
- [25] M.T. Carter, M. Rodriguez, A. Bard. *J. Am. Chem. Soc.*, **111**, 8901 (1989).
- [26] J.B. Chaires, N. Dattagupta, D.M. Crothers. *Biochemistry*, **21**, 3933 (1982).
- [27] A.E. Friedman, J.C. Chambron, J.P. Sauvage, N.J. Turro, J.K. Barton. *J. Am. Chem. Soc.*, **112**, 4960 (1990).
- [28] S. Satyanarayana, J.C. Dabrowiak, J.B. Chaires. *Biochemistry*, **31**, 9319 (1992).
- [29] G. Cohen, H. Eisenberg. *Biopolymers*, **8**, 45 (1969).
- [30] T. Mosmann. *J. Immunol. Methods*, **65**, 55 (1983).
- [31] K.K. Lo, T.K. Lee, J.S. Lau, W.L. Poon, S.H. Cheng. *Inorg. Chem.*, **47**, 200 (2008).
- [32] E.A. Steck, A.R. Day. *J. Am. Chem. Soc.*, **65**, 452 (1943).
- [33] J.E. Coury, J.R. Anderson, L. McFail-Isom, L.D. Williams, L.A. Bottmley. *J. Am. Chem. Soc.*, **119**, 3792 (1997).
- [34] Z.H. Liang, Z.Z. Li, H.L. Huang, Y.J. Liu. *J. Coord. Chem.*, **64**, 3342 (2011).
- [35] K.A. Kumar, K.L. Reddy, S. Satyanarayana. *J. Coord. Chem.*, **63**, 3676 (2010).
- [36] F.H. Wu, C.H. Zeng, Y.J. Liu, X.Y. Guan, L.X. He. *J. Coord. Chem.*, **62**, 3512 (2009).
- [37] J.G. Liu, Q.L. Zhang, X.F. Shi, L.N. Ji. *Inorg. Chem.*, **40**, 5045 (2001).
- [38] J.K. Barton, A.L. Raphael. *J. Am. Chem. Soc.*, **106**, 2466 (1984).
- [39] Y.J. Liu, Z.Z. Li, Z.H. Liang, J.H. Yao, H.L. Huang. *DNA Cell Biol.*, **30**, 839 (2011).
- [40] T.F. Chen, Y.N. Liu, W.J. Zheng, J. Liu, Y.S. Wong. *Inorg. Chem.*, **49**, 6366 (2010).
- [41] Y.J. Liu, Z.H. Liang, Z.Z. Li, H.L. Huang. *DNA Cell Biol.*, **30**, 829 (2011).